NJC

Accepted Manuscript

This article can be cited before page numbers have been issued, to do this please use: M. R. P. Kurup, N. Mohan, S. S S and S. B. Perakath, *New J. Chem.*, 2018, DOI: 10.1039/C8NJ02657B.

ROYAL SOCIETY OF CHEMISTRY

rsc.li/njc

ROYAL SOCIETY OF CHEMISTRY
View Article Online
DOI: 10.1039/C8NJ02657B

Journal Name

ARTICLE

Dual Responsive Salen-type Schiff Bases for the Effective Detection of L-Arginine *via* Static Quenching Mechanism.

Nithya Mohan,[a] S. S. Sreejith,[a] P. M. Sabura Begum [a] and M. R. Prathapachandra Kurup*[a,b]

Received 00th January 20xx,
Accepted 00th January 20xx

DOI: 10.1039/x0xx00000x

www.rsc.org/

L-Arginine is one of the most important amino acid and plays a key role in diagnostic studies. Herein we report four Salen-type Schiff base fluorimetric/colorimetric sensors for the rapid detection of L-arginine. Substituents play a major role in the sensing mechanism of the probes with the nitro-substituent bearing probe showing the highest efficiency. Evidence of a 1:2 complexation between all the probes and the analyte was evidenced from the absorption titrations; and the fluorescence studies revealed quenching phenomenon occurring during complex formation. From the life time measurements, the nature of quenching was found to be static and the formation of a ground state complex was confirmed. DFT calculations done at B3LYP/TZVP level of theory corroborated the experimental findings and further established the proton transfer happening from probe to the analyte during the complex formation.

Introduction

L-Arginine is the most propitious, naturally occurring amino acid among the non-thiol containing amino acids. The most inimitable property of Arginine among the rest of the natural amino acids is the high basicity of one of its terminal position *i.e*. guanidine part.[1] Its pKa value is found to be 13.8 and is a conditionally essential amino acid.[2] It is also found in cerebral system in 14µM concentration and has the highest isoelectric point[3]. Studies especially sensing appertaining to the detection of L-Arginine(L-Ar) has inordinate importance in the scientific community as well as in the medical and biological fields[4]. Arginine is one of the most important diagnostic indicator for some of the human diseases like hypertension, renal damage and also the varying concentration of Arginine or its derivatives cause many health issues that can even lead to death.[5, 6] Administration of L-Ar orally on patients with preeclampsia was found to accelerate foetal gain and improve biophysical profile.[7] Arginine also plays a pivotal role in the pathophysiology of hyperammonemia disorders and astrocytes of aggregating neural cell culture.[8]

Biological functions of Arginine include secretion of certain hormones such as insulin growth hormone, glucagon and prolactin.[9] It also has a vital role in cell division, healing of wounds *etc*. Nitric oxide which has many biological functions is also produced from the conversion of L-Arginine into Citrulline.[10] Besides these, some cell-cell, signalling molecules are also generated from Arginine in the presence of oxygen. Owing to its ability to attain different charge states, Arginine is involved in a large number of crucial biochemical process which includes some steps of metabolic pathways, trans-membrane transport *etc*. Also, Arginine is essential for the quantum chemical study of the interactions involved in proton transfer and other selective binding processes.[1, 2]

Extensive methods are available in the literature for the selective detection of Arginine. Apart from the voluminous data of detecting Arginine using methods like HPLC, mass spectrometry *etc*. Reports are there in the literature for the detection of thiol-containing amino acids using fluorescent probes. Fluorescent sensors for the detection and sensing of amino acids other than thiol-based ones are limited in number and still limited when it comes to colorimetric as well as fluorescent sensors.[11-13]

Among the reported sensors colorimetric detection are mainly reported in the field of gold based nano particles, which again has a limitation *i.e.* incorporation of costly Au particles.[9, 14, 15] Works including fluorescent, electrochemical and surface plasmon resonance detection of Arginine were reported but the sensor or probe used for this purpose are mainly of macrocyclic type like crown ether and quantum dots (QDs).[3, 16-18] These methods also bear some unavoidable limitations such as poor solubility, advanced experimental set up, sophisticated characterization methods and the use of costly metals. Recently colorimetric as well as fluorescent probes were

[a] Department of Applied chemistry
Cochin University of Science and Technology
Kochi, Kerala-682022, India
E-mail: mrpcusat@gmail.com.
[b] Department of chemistry, School of Physical Sciences
Central University of Kerala
Riverside Transit campus, Neeleshwar, Kerala-671314, India.
E-mail: mrp@cukerala.ac.in.

† Footnotes relating to the title and/or authors should appear here.
Electronic Supplementary Information (ESI) available:
IR, UV-VIS ^{1}H-NMR spectra, GC-MS data, crystal data refinement table and, hydrogen bonding interactions, Jobs plots, life-time data, K_{SV} value and Stern-Volmer plot, fluorimetric response times. CCDC 1845374 contain the supplementary crystallographic data for this paper. These data can be obtained free of charge via www.ccdc.cam.ac.uk/conts/retrieving.html or from the Cambridge Crystallographic Data Centre, 12 Union Road, Cambridge CB2 IEZ, UK; fax: (+44) 1223-336-033; or e-mail: deposit@ccdc.cam.ac.uk.] [details of any supplementary information available should be included here]. See DOI: 10.1039/x0xx00000x

View Article Online
DOI: 10.1039/C8NJ02657B

developed for the selective detection of Arginine, but none of them were able to propose the mechanism behind the sensing.[19, 20] These also fail in explaining the effect/presence of Arginine in the excited state life time of the probe. Also, the reason behind the quenching of fluorescent intensity of the probe is still unknown.

Through this work, we propose a Salen-type bicompartmental Schiff base systems for the effective sensing of the amino acid L-Arginine. To date, to the best of our knowledge, this is the first reported Salen-type system for the colorimetric detection of L-Arginine even though there are reports on the use of Schiff bases and its metal complexes for the sensing of cations and anions *etc.*[21-25] But the number is still limited in salen like systems.[26] The proposed detection technique is rapid, facile, cost effective and also has high selectivity.

Experimental

Materials.

2-Hydroxy-3-methoxybenzaldehyde, 5-Bromo-2-hydroxy-3-methoxybenzaldehyde, 5-Nitro-2-hydroxy-3-methoxybenzaldehyde, Ethylene diamine and L- Arginine were purchased from Sigma-Aldrich Chemical Co. Pvt. Ltd.; 2,2'-dimethyl ethylene diamine was purchased from Nice Chemicals Pvt. Ltd. and used as received. Fluorescein and Quinine sulphate were bought from LobaChemie Private Ltd., The stock solution of L-Arginine was prepared in distilled water. All other solvents and chemicals used were of analytical grade.

Physical Measurements

Elemental analyses and GC-MS data were collected from a Vario EL III CHNS elemental analyzer and using Trace 1300 GC and ISQ QD single quadruple GC-MS instrument respectively. IR spectra of the compounds were recorded on a JASCO FT-IR-5300 Spectrometer in the range 4000-400 cm^{-1} using KBr pellets. Electronic spectra of the compounds were taken on a Thermo scientific Evolution 220 spectrophotometer in the 260-700 nm range. Emission and lifetime measurements were taken using 530 nm laser source in Fluorolog and Flurolog TCSPC, Horiba Scientific respectively. ^{1}H NMR spectra of all the ligands except compound **2** and **4** were recorded from Bruker AVANCE II 500 NMR Spectrometer using $CDCl_3$ and compound **2** and **4** in d_6-DMSO.

Single-crystal X-ray diffraction measurement were performed on a Bruker SMART APEX diffractometer, equipped with a graphite crystal incident-beam monochromator, and a fine focus sealed tube with Mo Kα (λ = 0.71073 Å) as the X-ray source. The unit cell dimensions were measured and data collection was performed at 293(2) K. Data acquisition and integration were done using Bruker SMART and Bruker SAINT software[27]. Absorption corrections were carried out using SADABS based on Laue symmetry using equivalent reflections[28]. The structure was solved by direct methods and refined by full-matrix least-squares calculations with the SHELXL-2016/1 software[29]in the WINGX software package[30]. The structures were plotted using the graphics tools DIAMOND version 3.2 k[31] and ORTEP-3 for windows[30].All the C bound H atoms were derived from Fourier difference maps and were placed geometrically (C–H = 0.98-0.99 Å) and refined in the riding model approximation with U(H) set to 1.2 U (C) (1.5 U for CH_3). Anisotropic displacement parameters of C6 and C7 were restrained using enhanced rigid bond restrain for the 1,2 distances using RIGU command and some reflections were omitted owing to disagreement.

Synthesis and characterization of the compounds

In order to study the structural effect of Salen type Schiff base compounds, we have synthesized four different types of compounds by changing the substitution at the salicylaldehyde moiety as well as in the spacer groups. Compounds **1** to **4** were synthesized according to the route shown in Scheme 1.

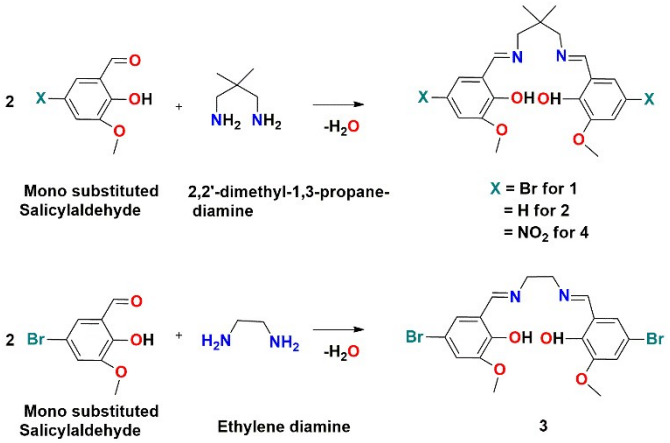

Scheme 1 Synthetic route for the formation of Schiff bases.

Compound **1** was synthesized by the addition of a methanolic solution of 2,2'–dimethyl-1,3-propane diamine into a round bottom flask containing 5-bromo-3-methoxy-2-hydroxy salicylaldehyde in methanol.[32] A fluorescent yellow colored solution was formed immediately after the addition of diamine. The reaction mixture was refluxed using simple water condenser at a temperature of 50 °C for 2 hours.[33] Yellow colored product formed was filtered, washed with methanol and recrystallized from DMSO. Purification method adopted here is recrystallization instead of chromatography since degradation of Schiff base happens during the purification step through hydrolysis.[26] Same method was adopted for the syntheses of other compounds: **2** to **4**. Diffraction quality single crystals were obtained for **2** after recrystallization of the precipitate from DMSO. Immediate precipitation was observed in the case of **3** and **4** respectively. The precipitate was collected and washed with methanol and recrystallized in DMSO solvent.

Compound **1** : Yield (73%); ^{1}H NMR (500 MHz, $CDCl_3$,TMS): δ 14.84 (s, –OH, 2H), δ 8.24 (s, 2H), δ 6.90 – 7.01 (m, Aromatic Protons 4H), δ 3.91 (s, $-OCH_3$, 6H), δ 3.49 (d, 4H), δ 1.07 (s, 6H), (Fig S1, ESI†). FTIR/cm^{-1} (KBr): 3481 (–OH), 2982 (CH_{st}), 1613 (C=N), 1472(Ar C=C), 1229 (C-O), (Fig. S2, ESI†). GC-MS: 528.94 (M+2, 100%) (Fig. S3, ESI†). Anal.calc. (%) for $C_{21}H_{24}Br_2N_2O_4$: C, 47.75; H, 4.58;N, 5.30. Found (%) C, 47.35;H,4.61; N, 5.31.

Compound **2** : Yield, (70%); ^{1}H NMR (500 MHz, DMSO,TMS): δ 14.09 (s, –OH, 2H), δ 8.47 (s, 2H), δ 6.9 – 7.01 (m, Aromatic Protons 4H), δ 3.74 (s, –OCH_3, 6H), δ 3.45 (d, 4H), δ 0.95 (s, 6H), (Fig S1, ESI†). FTIR/cm^{-1} (KBr): 3441 (–OH), 2982 (CH_{st}), 1633 (C=N), 1465(Ar C=C), 1249 (C-O), 736(C-Br), (Fig. S2, ESI†). GC-MS: 371.23 (M+1, 100%) (Fig. S3, ESI†). Anal.calc. (%) for $C_{21}H_{26}N_2O_4$: C, 68.09; H, 7.07;N, 7.56. Found (%) C, 68.23;H,7.09; N, 7.27.

Compound **3** : Yield, (86%); ^{1}H NMR (500 MHz, DMSO,TMS): δ 13.57 (s, –OH, 2H), δ 8.23 (s, 2H), δ 6.9 – 7.2(m, Aromatic Protons 4H), δ 3.88 (s, –OCH_3, 6H), δ 3.96 (t, 4H), (Fig S1, ESI†). FTIR/cm^{-1} (KBr): 3420 (–OH), 2928 (CH_{st}), 1617 (C=N), 1459(Ar C=C), 1235 (C-O), 689(C-Br), (Fig. S2, ESI†). GC-MS: 485.92 (M+2, 100%) (Fig. S3, ESI†). Anal.calc. (%) for $C_{18}H_{18}Br_2N_2O_4$: C, 44.47; H, 3.73; N, 5.76. Found (%) C, 44.62; H, 3.76; N, 5.33.

Compound **4** : Yield (82%); mp, 212 °C. ^{1}H NMR (500 MHz, DMSO,TMS): δ 14.2 (s, –OH, 2H), δ 8.58 (s, 2H), δ 7.27 – 7.94 (m, Aromatic Protons 4H), δ 3.76 (s, –OCH_3, 6H), δ 3.63 (t, 4H), δ 1.1 (s, 6H) (Fig S1, ESI†). FTIR/cm^{-1} (KBr): 3420 (–OH), 2955 (CH_{st}), 1654 (C=N), 1532 (Assy. NO_{2st}), 1317 (Sym. NO_{2st}), 1438(C-N), 1256 (C-O), (Fig. S2, ESI†). GC-MS: 485.92 (M+2, 100%) (Fig. S3, ESI†). Anal.calc. (%) for $C_{21}H_{24}Br_2N_4O_8$: C,54.78; H, 5.25; N, 12.17. Found (%) C, 54.44; H, 5.28; N, 12.31.

Colorimetric sensing of L-Arginine

UV-Vis titration measurements.

Stock solution of compound **1** (sensor/probe **1**) was prepared in 10^{-3} M (0.0052 g in 10 mL) concentration in DMSO solvent. It is then diluted to obtain a concentration of 10^{-5} M. The analyte L-Ar was prepared in distilled water having a concentration of 10^{-3} M (0.0017 g in 10mL). From this a volume of 2500 µL was pipetted out into a 25 mL std. flask and made up to the mark in order to obtain a concentration of 10^{-4} M. Colorimetric response was studied by the addition of 100 µL of analyte into a cuvette containing 100 µL of the sensor, it is then diluted to a total volume of 2 mL. An immediate color change from colorless to light yellow was observed. The UV spectra were then recorded at room temperature. The titration experiment was conducted with the addition of L-Ar in the volume range of 20 – 200 µL.

The same procedure was adopted for the colorimetric sensing of L-Ar using compounds **1** to **3** (Fig. 2). The concentration of compound **4** (sensor **4**) was reduced to 10^{-6} M since it shows a higher optical density than the other ones. This is an indication of its higher sensitivity towards our interest *ie*. L-Ar.

Selectivity test

Prior to the above absorption titration measurements, competition tests were performed with 5 equivalents of fourteen amino acids (Gly, Ala, Lys, Trp, Arg, Val, His, Leu, Ph ala, Ser, Asp, Cys, Tyr and Glu (Fig. S4)).

Job's plot Analysis.

Job's Plot analysis was done by adding 5 to 50 µL of L-Ar solution to a quartz cuvette containing 100 µL of the sensor and the total volume was made to 2000 µL. The UV spectra of the sensor–L-Ar mixture were recorded separately and the Job's Plot were drawn to confirm the composition of adduct formed.

Fluorescence studies

Fluorometric Titration

In order to study the fluorescence spectral response of the synthesized sensors towards L-Ar, fluorescence titration was performed with the probe and the analyte in a concentration same as above. But the addition of the analyte was little bit different *i.e* 10 to 150 µL since this method is much more sensitive than the absorption titration.

Lifetime Measurement

The Lifetime measurement was carried out to study the mechanism behind the sensing of L-Ar by the synthesized sensors using a 530 nm laser source. The study was conducted with and without the analyte L-Ar and the plot was constructed with counts against time of decay. Stern-Volmer plots were analyzed to confirm the mechanistic route for the detection of analyte.

NMR Titration Experiment

^{1}H NMR titration with single addition of L-Ar was carried out in probes **2** and **4**. NMR spectrum of each probe was recorded individually and 2 equivalents of the analyte was added to the probes **2** and **4** in order to study the change as well as the interacting part of the probe. To carry out the experiment, **2** and **4** were dissolved in d_6-DMSO and the analyte was dissolved in D_2O solvent. The solvent d_6-DMSO was chosen for the experiment in order to avoid the possibility of solvent exchange of OH protons with the added D_2O solvent.

Theoretical Calculations

DFT calculations were done employing ORCA 3.0.3 software package[34, 35] using the Becke's three-parameter hybrid exchange functional including the Lee–Yang–Parr nonlocal correlation functional (B3LYP)[36, 37] and the triple zeta valence basis set with one set of polarization function (TZVP)[38]. To accelerate the calculations, the resolution of identity (RI) approximation was utilized with the decontracted auxiliary def2–TZV/J Coulomb fitting basis sets and the chain–of–spheres (RIJCOSX) approximation to exact exchange as implemented in ORCA.[39] Initial geometries used for the optimization process were taken either from crystal structure or from NMR results. The optimized geometries were then confirmed to be global energy minima by performing frequency calculations which returned no imaginary frequency. TZVP basis set was used since it reduces the basis set superposition error (BSSE) to negligible in the calculation of systems with noncovalent interactions. Avogadro software was used for the visualization of orbitals.[40]

Results and Discussion

Crystal structure description of 2

The asymmetric unit of the compound consists of a single molecule having the molecular formula $C_{21}H_{26}N_2O_4$. It crystalizes into monoclinic $P2_1/n$ space group (Table S1). The torsional angle between C1–C7–N4–O8 was found to be 178.74(2)° which suggests an *E* conformation of the molecule w.r.t. the azomethine nitrogen atom. The two terminal moieties including the benzene ring of the aldehydic parts lie nearly in a perpendicular fashion as evident from the angle measured between the two planes which returned a value of 124°. The two intramolecular hydrogen bonding interactions (O(2)–H(2)··· N(1) and O(3)–H(3)··· N(2)) present in the crystal system results in the formation of S(6) ring motifs and also adds to the stability of the solid structure of the compound (Fig 1b, Table S2).[41, 42] One of the azomethine nitrogen atom N(2) acts as an acceptor in the intramolecular nonclassical hydrogen bonding interaction (C(11)–H(11)··· N(2)) which results in the formation of S(5) ring motif. Thus N(2) forms a bifurcated hydrogen bond with two different donor atoms *i.e.* O(3) and C (11) (Fig1b). The ORTEP image including the numbering scheme of **2** is shown in Figure 1a.

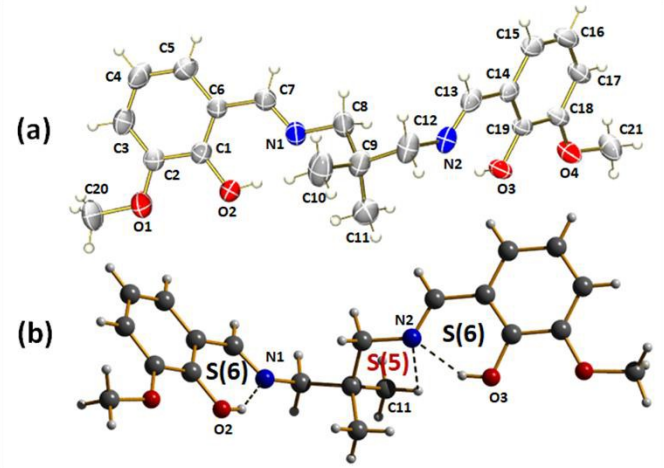

Figure 1 (a) ORTEP diagram of **2** with atom numbering scheme (for clarity hydrogen atoms are not labelled); (b) Intramolecular hydrogen bonding interactions generating two types of ring motifs.

Sensors **1** to **4** were synthesized, initially characterized and were subjected to absorption titrations to study their sensing ability towards L-Arginine (L-Ar). The absorption peak around 331 nm in sensor **1** was found to significantly decrease with the incremental addition of the analyte and a concomitant increase in absorbance at 418 nm was also found. Absorbance @418 nm is the newly formed band and was absent in the sensor which also gave the initial experimental proof for (sensor + L-Ar) complex formation. As the phenolic OH groups in the sensor are acidic in nature, it gets deprotonated in presence of a strongly basic analyte L-Ar. Hence this band may be attributed to the deprotonation of the probe in presence of the strong base L-Ar.[19] In addition to the new band, a clear isosbestic point was noted at 315 nm which also gave the evidence for the existence of the complex/adduct formation. In addition to the above observation, it was very interesting to observe the color change of the probe from colorless to light yellow which makes it a colorimetric naked eye sensor. It is worth mentioning that the naked eye detection was viable only at relatively high L-Ar concentration.

The sensors reported here (**1** to **4**) show a similar pattern in the absorption titration curves but the position of the newly formed peak and isosbestic points were shifted accordingly with the substituents on the aldehydic as well as the diimine spacer part (Fig 2). Apart from competitive experiments, analogous investigations were carried out using absorption titration method with alanine but the response was negligible and could be ignored.

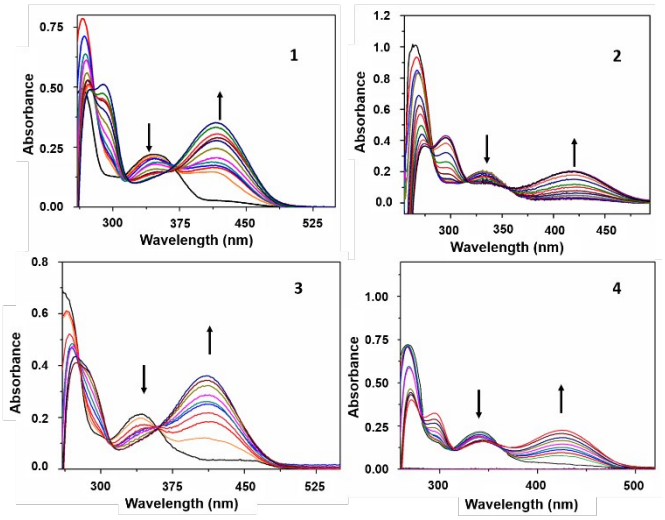

Figure 2 Absorption titration curves of sensors **1**-**4** with incremental addition (20-200 µL) of L-Arginine.

In order to probe into the stoichiometry of the complex formed, Jobs plot analysis were done and the ratio was found to be 1:2 (sensor: L-Ar) for all the four sensors. The mass data also support the result from the jobs plot (Fig S5). Initially the m/z peak observed for sensor **1** at 528.94 corresponds to m+2. When 2 equivalents of L-Ar was added to the sensor, new m/z peak was found in consonance with that of (**1** + 2 L-Ar) (Fig S6).

The sensors are then subjected to fluorescent titration measurements and quenching of fluorescence was observed when L-arginine was added to the fluorescent probe (Fig 3). Recent reports on Salen Schiff bases discusses anion or amino acid sensing via fluorescence enhancement.[43, 44] Similarly a new type of emission enhancement called aggregation-induced emission (AIE) is also reported.[45, 46] The two enhancement phenomenon are entirely different, as in the case of anion/amino acid sensing the fluorescence enhancement is due to the uniform distribution of π-function Frontier molecular orbitals in the molecule skeleton. While in AIE it is originated from aggregated molecules in its solid state or in H_2O due to weak intermolecular face–face π···π interactions, multiple hydrogen bonds and other strong non-covalent intermolecular interactions between adjacent moieties. In contrast, in this work, the quenching may be due to the intermolecular proton transfer between the sensor and the L-Ar.[47] To explore this

quenching phenomena, life time measurement was done in each sensor and also with its analyte (see later).

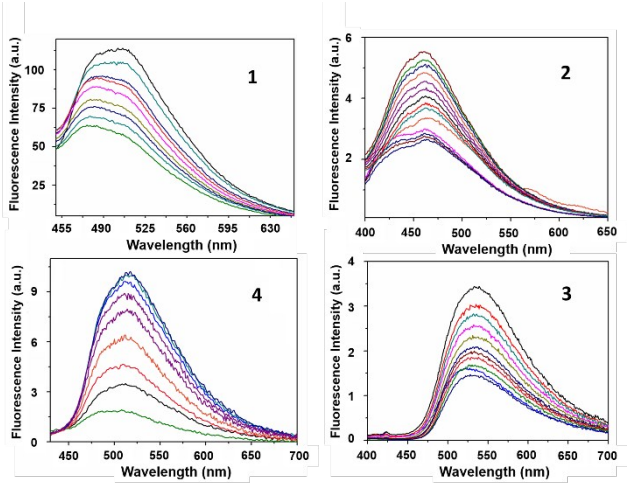

Figure 3 Quenching of emission intensity in compounds **1**-**4**.

The most important facets of a sensor are its ability for the rapid detection of an analyte and its stability. This was confirmed by measuring the fluorescence intensity at different time intervals after the initial scan and it was noticed that the intensity remains constant after 12-14 seconds (Fig S7). This immediate time response towards the analyte may increase its practical utility. Among the four sensors, sensor **4** became stable after 12 seconds even though the concentration of **4** is lower than that of the rest (Fig S7). Further sensitivity of probes was measured and **4** exhibited the lowest detection limit of 1×10^{-6}molL^{-1}.

Mechanism of Sensing

Complex or adduct formation of the sensor with the analyte was confirmed from the UV-Vis absorption titration studies. Further to explore the reason behind sensing/recognition of analyte and quenching of fluorescence, life time measurements were done. There are reports explaining the sensing mechanism of analyte by life time study. But to the best of our knowledge, this is the first reported salen system which senses arginine and also the method employed here (life time study) is hitherto unexplored to investigate mechanism in these class of systems. Fluorescence life time method is not only the most reliable one but is an accurate method to get an insight into the mechanistic pathway of a reaction.[48, 49] The quenching may be due to the excited-state reactions, molecular rearrangements, ground-state complex formation, collisional quenching, energy/electron transfer and emission group destruction etc. There are two important types of fluorescent quenching, first is the collisional/ dynamic quenching and second is the static quenching. For either static or dynamic quenching to occur, the fluoro probe and the quencher must be in contact with each other.[50] Dynamic quenching may be attributed to the nonradiative electron transfer from the excited state of the fluoroprobe to the analyte molecule. Due to its diffusion-controlled collision, change in life time may be observed and also it affects only the excited states of the fluorophores, and thus no changes in the absorption spectra after the addition. On the other hand, static quenching may occur due to the formation of a complex between the fluorophore and quencher. When this complex absorbs light it immediately returns to the ground state without emission of a photon and the observed fluorescence is from the non-complexed fluorophores. In this case, the life time of the sensor will remain unchanged even after the addition of an analyte and $\tau_0/\tau = 1$, where τ_0 and τ are life time of the probe and mixture respectively.[51]

To investigate the quenching behaviour and thereby the underlying mechanism of recognition, lifetime measurements of the probe was done with and without the addition of analyte L-Ar. The average life time was calculated and it was observed that the life time remains unchanged even after the addition of L-Ar (Table S3, Fig 4). The above discussed spectroscopic results reveal the existence of a static type of quenching and the formation of a non-emissive ground state complex. To get further insight into the type of quenching, we analysed the UV-Vis spectra of the probe and the mixture (Probe + L-Ar) carefully. The obtained UV-Vis spectra are in good agreement with the static quenching mechanism for our proposed sensors since the UV-Vis spectra for the mixtures obtained through incremental addition of arginine consists of a new peak and the presence of isosbestic points confirms the formation of a ground state complex.[52]

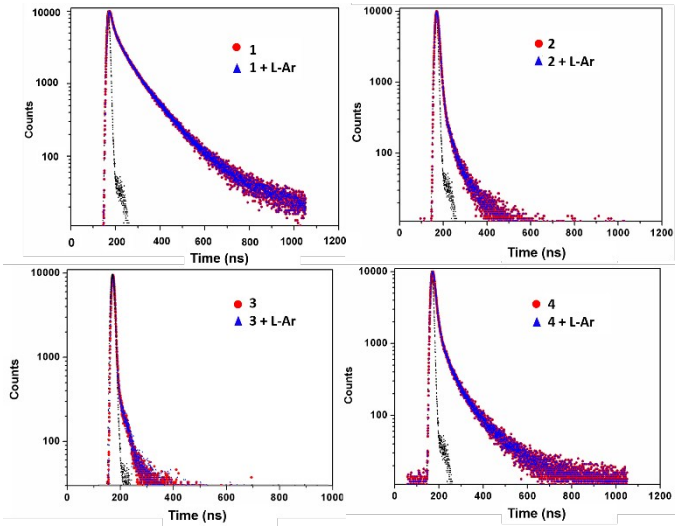

Figure 4 Life time plots of sensors **1**-**4** and their respective mixture with L-arginine.

The static fluorescent quenching was further analysed with the Stern-Volmer equation

$$I_0/I = K_{SV}[Q] + 1$$

Where,

I_0 = fluorescent intensity of the sensor before the addition of the analyte

I = fluorescent intensity after the addition of the analyte

K_{SV} = Stern-Volmer constant

[Q] = molar concentration of the analyte (M^{-1}).

The Stern-Volmer (SV) plots show good agreement with the static type of quenching and ground state interaction of the

probe and the analyte with **4** having the highest K_{SV} value (Fig. S8, Table S4 in ESI).

As all the sensors have two acidic moieties (two phenolic OH) and the analyte is a strong base, there is a high chance of complex/adduct formation through proton transfer.[47] ^{1}H-NMR experiments were performed for its verification. To elucidate the deprotonation, 1 eqv. of L-Ar (D_2O) was added to the sensor and the ^{1}HNMR spectra of the sensor **2** and **4** were then recorded in d_6-DMSO solvent before and after the addition. DMSO solvent was selected so as to avoid the D_2O exchange. The OH peak was found to be absent in the NMR spectrum of the mixture containing (sensor **2** + L-Ar) confirming the proton transfer and involvement of OH group in the complex formation (Fig. 5). From the literature survey also, it was clear that the amino acid L-arginine is a strong base having a pKa value of 13.8 and is strong enough to deprotonate these OH groups.

It can be proposed that the sensing mechanism involves the complex/adduct formation between the acidic part of the sensors and the basic part of the arginine. Since there is no major difference in the structure between the sensors, we can explain the mechanism by taking the example of sensor **1**. The complex formation is initiated by the proton transfer of the acidic phenolic OH by the basic NH group of the guanidine part of the arginine (Scheme 2). This results in the formation of slightly negative charge at the proximity of the phenolic oxygen which in turn attracts the guanidine part of the arginine where now there is a slight positive charge formation due to the aforementioned proton transfer. This is also evidenced from ^{1}HNMR where the OCH_3 protons due to their position near to the negative charge of the adduct are downfield shifted (Fig 5). Proper orientation of –OH and –OCH_3 plays a significant role in the recognition of L-Ar. The deprotonated ArO^- form is stabilised by the presence of electron donating –OCH_3 which is critical in the formation of the adduct/complex. It does not mean that these functionalities are mandatory for the sensing of an amino acid since in some other systems where there is no –OCH_3 group, sensing happens but the interaction is somewhat different.[43, 47]

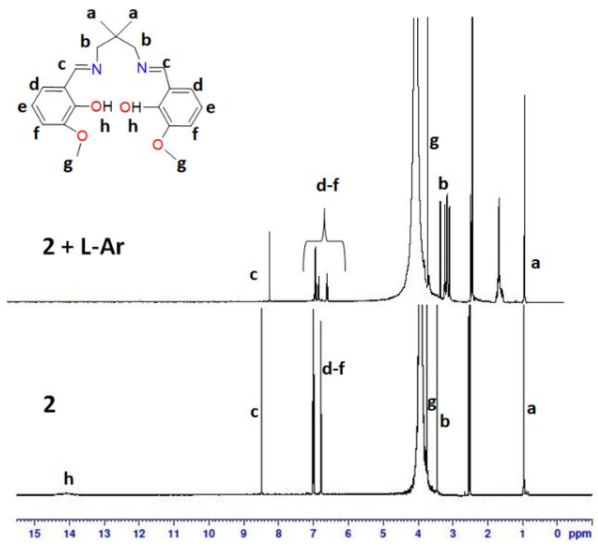

Figure 5 NMR plots of **2** alone and after the addition of 1 equivalent of L-arginine.

Since the guanidine part in L-Ar is more basic, more probable interacting part with the acidic part of the sensor will be the guanidine terminal. The hypothesis of guanidine part interacting in the complex/adduct formation was verified by performing absorption titration. For confirming this, the absorption titration was performed with guanidine hydrochloride and the spectra obtained was exactly similar to that of the Sensor-L-Ar spectra (Fig S9).

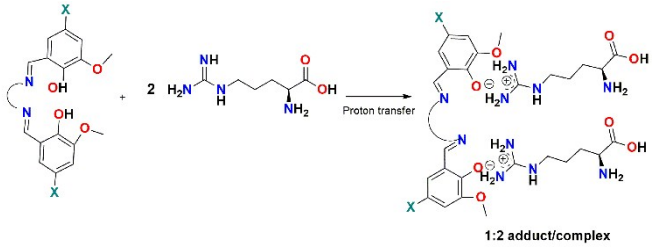

Scheme 2 Formation of 1:2 adduct via proton transfer from probe to the analyte.

Experimentally obtained results and the proposed mechanism were further verified by performing DFT calculations of the compounds at the B3LYP/def2-TZVP level of theory. To find out the plausible stable complex, the frontier orbitals of the optimized geometries of all the Salen Schiff bases (**1**-**4**) and the arginine analyte were compared (Table 1, Fig 6). It was found that among the probes, **4** has the most stabilized LUMO (-2.339 eV) which means that it is the strongest acid[53] and the LUMO is concentrated on the phenol moieties on both the sides (Fig 6) (For details about orbital composition see ESI). This electrophilic nature of **4** helps in the effective proton transfer to the analyte retaining its negative charge. This results in the formation of a **4**-L-Ar (1:2) ground state complex (Scheme 2). This is obvious since the presence of electron withdrawing nitro group in the para position to the phenolic OH on both aldehydic moieties in **4** helps in the deprotonation thereby attaining a negative charge in the complex/adduct (Scheme 2).

From the table 1, it can be seen that the second most stabilized LUMO is that of **2** (-2.274 eV) but its HOMO is having the highest energy (-4.056 eV) among the selected probes which results in a strong basic nature. For the two bromo substituted compounds **1** and **3** the LUMO values are comparable with each other (-1.513 and -1.484 eV) and higher than that of **4** and **2**. But the low energy for HOMO in both **1** and **3** (-5.858 and -5.713 eV) when compared to that of **2** results in low nucleophilicity and a better overall acidic character than that of **2**. Thus, the theoretical calculations substantiate the experimental observations whereby the effective proton transfer to the analyte follows the order **4**>**1**>**3**>**2**.

Table 1 HOMO-LUMO energies calculated for the probes and L-arginine at B3LYP/TZVP level of theory

Compounds	HOMO(eV)	LUMO(eV)	Band Gap(eV)
Arginine	-6.106	0.130	-6.236
1	-5.858	-1.513	-4.345
2	-4.056	-2.274	-1.782
3	-5.713	-1.484	-4.229
4	-5.995	-2.339	-3.656

Conclusions

Herein we report novel Salen-type Schiff bases for the recognition and sensing of biologically important amino acid L-Arginine. These are the first reported Salen-type systems for both fluorimetric and colorimetric sensing of L-Arginine in aqueous solution. Among the tested probes the one with nitro substituent in the aldehydic moiety showed the highest sensing character which shows the effect of substituents on the sensing ability. Studies carried out using absorption titrations confirmed the formation of 1:2 complex between respective probes and L-arginine. Further fluorescence quenching measurements and life time studies revealed static quenching and the formation of a ground state complex. The experimental results are substantiated with DFT calculations involving frontier orbitals performed at B3LYP/TZVP level of theory which shows the possibility of proton transfer during complex formation. The facile synthetic procedure and appreciable detection limit of the synthesized probes make them cheap and practical sensors for L-arginine. We believe that this work will serve as a foundation for further investigations on the use of these class of compounds as biologically important sensors.

Conflicts of interest

There are no conflicts to declare.

View Article Online
DOI: 10.1039/C8NJ02657B

Acknowledgements

NM is thankful to Cochin University of Science and Technology and UGC-SAP for the financial assistance. NM acknowledges Prof. S. Prathapan and Dr. N. Manoj for their timely help. The authors are thankful to SAIF-CUSAT, NIIST-Trivandrum for various analyses.

Notes and references

1. M. Song, Z. Sun, C. Han, D. Tian, H. Li and L. Jiang, *Chem. Eur. J.*, 2014, **20**, 7987-7993.
2. J. R. Avilés-Moreno, G. Berden, J. Oomens and B. Martínez-Haya, *Phys. Chem. Chem. Phys.*, 2017, **19**, 31345-31351.
3. H. Liu, M. Li, L. Jiang, F. Shen, Y. Hu and X. Ren, *Spectrochimi. Acta A.*, 2017, **173**, 105-113.
4. G. C. Ligthart-Melis and N. E. Deutz, *Am. J. Physiol.Endocrinol. Metab.*, 2011, **301**, E264-E266.

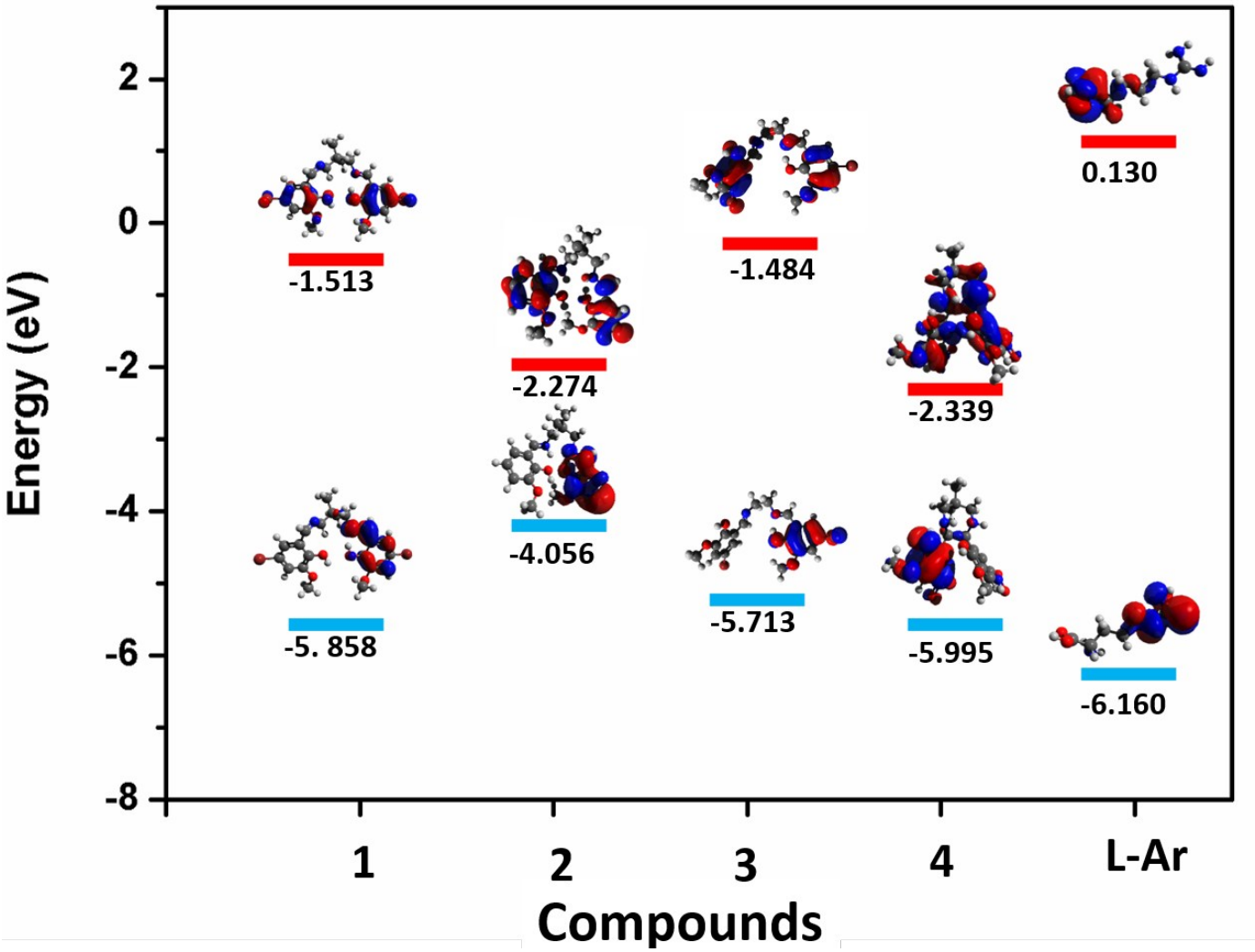

Figure 6 HOMO-LUMO plots and energy levels of the probes and analyte calculated at B3LYP/TZVP level of theory.

5. L. He, V. L. L. So and J. H. Xin, *Sens. Actuators B, Chem.*, 2014, **192**, 496-502.
6. N. Verma, A. K. Singh and M. Singh, *Biochem. Biophys.Rep.*, 2017, **12**, 228-239.
7. K. Rytlewski, R. Olszanecki, R. Lauterbach, A. Grzyb and A. Basta, *Basic Clin. Pharmacol. Toxicol.*, 2006, **99**, 146-152.
8. M. Morita, T. Hayashi, M. Ochiai, M. Maeda, T. Yamaguchi, K. Ina and M. Kuzuya, *Biochem. Biophys. Res. Commun.*, 2014, **454**, 53-57.
9. Q. Qian, J. Hao, W. Ma, P. Yu and L. Mao, *Anal. Bioanal. Chem.*, 2016, **408**, 3005-3012.
10. M. B. Witte and A. Barbul, *Wound Repair Regen.*, 2003, **11**, 419-423.
11. J. Cao, L. Ding, W. Hu, X. Chen, X. Chen and Y. Fang, *Langmuir*, 2014, **30**, 15364-15372.
12. J. Cao, L. Ding, Y. Zhang, S. Wang and Y. Fang, *J. Photochem. Photobiol. A, Chem.*, 2016, **314**, 66-74.
13. J. Li, Y. Zhang, Y. Chen, X. Shang, T. Ti, H. Chen, T. Wang, J. Zhang and X. Xu, *J. Mol. Recognit.*, 2018, **31**.
14. G. Patel and S. Menon, *Chem. Commun.*, 2009, 3563-3565.
15. K. A. Rawat and S. K. Kailasa, *Microchim. Acta*, 2014, **181**, 1917-1929.
16. M. Wehner, T. Schrader, P. Finocchiaro, S. Failla and G. Consiglio, *Org. Lett.,*, 2000, **2**, 605-608.
17. Y. He, M. Xu, R. Gao, X. Li, F. Li, X. Wu, D. Xu, H. Zeng and L. Yuan, *Angew. Chem., Int. Ed.*, 2014, **53**, 11834-11839.
18. T. Grawe, T. Schrader, P. Finocchiaro, G. Consiglio and S. Failla, *Org. Lett.,*, 2001, **3**, 1597-1600.
19. A. Ghorai, J. Mondal and G. K. Patra, *New J. Chem.*, 2016, **40**, 7821-7830.
20. X. Shang, J. Li, K. Guo, T. Ti, T. Wang and J. Zhang, *J. Mol. Struct.*, 2017, **1134**, 369-373.
21. A. Kumar, M. Dubey, R. Pandey, R. K. Gupta, A. Kumar, A. C. Kalita and D. S. Pandey, *Inorg. Chem.*, 2014, **53**, 4944-4955.
22. J. Cheng, X. Ma, Y. Zhang, J. Liu, X. Zhou and H. Xiang, *Inorg. Chem.*, 2014, **53**, 3210-3219.
23. M. S. Kim, S. Y. Lee, J. M. Jung and C. Kim, *Photochem. Photobiol. Sci.*, 2017, **16**, 1677-1689.
24. A. Ganguly, B. K. Paul, S. Ghosh, S. Kar and N. Guchhait, *Analyst*, 2013, **138**, 6532-6541.
25. M. Köse, G. Ceyhan, M. Tümer, İ. Demirtaş, I. Gönül and V. McKee, *Spectrochimi. Acta A.*, 2015, **137**, 477-485.
26. J. Cheng, K. Wei, X. Ma, X. Zhou and H. Xiang, *J. Phys. Chem. C*, 2013, **117**, 16552-16563.
27. S. SMART, *Bruker Analytical X-ray, Madison, WI, USA*, 1997.
28. SADABS, *Bruker Analytical X-ray, Madison, WI, USA*, 1997.
29. G. M. Sheldrick, *Acta Cryst. C*, 2015, **71**, 3-8.
30. L. J. Farrugia, *J. Appl. Cryst.*, 2012, **45**, 849-854.
31. K. Brandenburg, *Crystal Impact GbR, Bonn, Germany*, 2010.
32. C. S. Yeap, H. Kargar, R. Kia and H.-K. Fun, *Act Cryst. E*, 2009, **65**, o20-o21.
33. N. Mohan, S. Sreejith, M. Sithambaresan and M. P. Kurup, *Act Cryst. E*, 2014, **70**, o182-o183.
34. F. Neese, *WIREs Comput. Mol. Sci.*, 2012, **2**, 73-78.
35. F. Neese, *Density Functional and Semiempirical Program Package, Version*, 2008, **2**.
36. A. D. Becke, *J. Chem. Phys.*, 1993, **98**, 5648-5652.
37. C. Lee, W. Yang and R. G. Parr, *Phys. Rev. B.*, 1988, **37**, 785.
38. A. Schäfer, H. Horn and R. Ahlrichs, *J. Chem. Phys.*, 1992, **97**, 2571-2577.
39. F. Weigend and R. Ahlrichs, *Phys. Chem. Chem. Phys.*, 2005, **7**, 3297-3305.

View Article Online DOI: 10.1039/C8NJ02657B

40. M. D. Hanwell, D. E. Curtis, D. C. Lonie, T. Vandermeersch, E. Zurek and G. R. Hutchison, *J. Cheminform.*, 2012, **4**, 17.
41. M. C. Etter, *Acc. Chem. Res.*, 1990, **23**, 120-126.
42. S. Sreejith, N. Mohan and M. P. Kurup, *Polyhedron*, 2017, **135**, 278-295.
43. G. Shen, F. Gou, J. Cheng, X. Zhang, X. Zhou and H. Xiang, *RSC Adv.*, 2017, **7**, 40640-40649.
44. X. Zhang, J. Shi, G. Shen, F. Gou, J. Cheng, X. Zhou and H. Xiang, *Mater. Chem. Front.*, 2017, **1**, 1041-1050.
45. J. Cheng, Y. Li, R. Sun, J. Liu, F. Gou, X. Zhou, H. Xiang and J. Liu, *J. Mater. Chem. C*, 2015, **3**, 11099-11110.
46. M. Wang, C. Cheng, J. Song, J. Wang, X. Zhou, H. Xiang and J. Liu, *Chin. J. Chem.*
47. S. D. S. Parveen, A. Affrose and K. Pitchumani, *Sens. Actuators B, Chem.*, 2015, **221**, 521-527.
48. S. Sanda, S. Parshamoni, S. Biswas and S. Konar, *Chem. Commun.*, 2015, **51**, 6576-6579.
49. Y. Song, S. Zhu, S. Xiang, X. Zhao, J. Zhang, H. Zhang, Y. Fu and B. Yang, *Nanoscale*, 2014, **6**, 4676-4682.
50. J. R. Lakowicz, in *Principles of fluorescence spectroscopy*, Springer, 1999, pp. 25-61.
51. F. Wang, Z. Gu, W. Lei, W. Wang, X. Xia and Q. Hao, *Sens. Actuators B, Chem.*, 2014, **190**, 516-522.
52. Y. Zhang, P. Cui, F. Zhang, X. Feng, Y. Wang, Y. Yang and X. Liu, *Talanta*, 2016, **152**, 288-300.
53. D. E. Lewis, *J. Chem. Educ.*, 1999, **76**, 1718.

View Article Online
DOI: 10.1039/C8NJ02657B

Effect of substituents of Salen Schiff bases on the detection of L-arginine via static quenching mechanism is discussed.